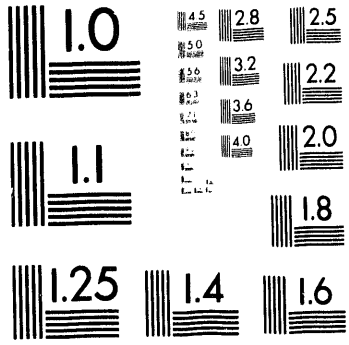
1.0
1.1
1.25
1.4
1.6
1.8
2.0
2.2
2.5
2.8
3.2
3.6
4.0
4.5
5.0
5.6
6.3
7.1

1 of 1

58918-00-105 Manuscript September 1993

Orientationally independent antiferromagnetic coupling in epitaxial Fe/Cr (211) and (100) superlattices*

Eric E. Fullerton, M.J. Conover, J.E. Mattson, C.H. Sowers, and S.D. Bader

Materials Science Division
Argonne National Laboratory, Argonne, IL 60439

jmc

*Work supported by the U.S. Department of Energy , Basic Energy Sciences-Materials Sciences, under contract #W-31-109-ENG-38.

Submitted: 38th Magnetism and Magnetic Materials Conference
November 15-18, 1993
Minneapolis, MN

Orientationally independent antiferromagnetic coupling in epitaxial Fe/Cr (211) and (100) superlattices*

Eric E. Fullerton, M.J. Conover, J.E. Mattson, C.H. Sowers, and S.D. Bader

Materials Science Division
Argonne National Laboratory
Argonne, IL 60439

We present structural and magnetic characterization of epitaxial Fe/Cr(211) and Fe/Cr(100) superlattices grown simultaneously on MgO(110) and MgO (100) substrates by magnetron sputtering. The epitaxial orientation of the Fe/Cr(211) superlattice with the MgO(110) substrate is Fe/Cr[$0\bar{1}1$] // MgO[001] and the orientation of Fe/Cr(100) is Fe/Cr[001] // MgO[011]. We find that for both orientations, that the interlayer coupling oscillates in sign with a period of 18Å, and, furthermore, that the strength and phase of the magnetic coupling are also nearly identical for these two orientations.

PACS #: 75.50.Rr, 75.30.Et, 68.55.-a

* Work supported by the U.S. Department of Energy, BES-Materials Sciences, under contract W-31-109-ENG-38.

I. Introduction

Oscillatory interlayer coupling across nonmagnetic spacer layers in ferromagnetic/nonmagnetic transition-metal multilayers[1-4] has become a challenging theoretical problem.[5-13] Most theories are based on a band-structure-modified RKKY treatment of the spacer layer. Within this framework, the oscillations in the coupling arise from spanning vectors normal to the layers which join extremal points of the bulk Fermi surface. The period of oscillation is inversely proportional to the length of the particular spanning vector giving rise to the coupling. Whereas the period is thought to be solely a property of the spacer material, the phase and strength of the coupling will also depend on the ferromagnetic material and structural aspects of the interface such as roughness and interdiffusion.[5-12] A stringent test of this approach is to study the interlayer coupling along different crystallographic directions of the spacer, since different spanning vectors should be probed for each orientation. This type of experiment has been performed most extensively for the Co/Cu system along the three low-Miller-index directions.[13-17] In this paper, we discuss the interlayer coupling of Fe/Cr(211) and (100) superlattices which have been epitaxially grown onto MgO (110) and (100) substrates respectively. We find that for both orientations, that the interlayer coupling oscillates in sign with a period of 18Å, and, furthermore, that the strength and phase of the magnetic coupling are also nearly identical for these two orientations.

II. Experimental Procedure

The Fe/Cr superlattices were grown by d.c. magnetron sputtering onto single-crystal MgO(110) and MgO(100) substrates. The sputtering chamber had a base pressure of $<5\times10^{-8}$ Torr and the sputtering guns were operated in an Ar pressure of 3 mTorr. The (110) and (100) substrates were mounted side-by-side onto the sample holder and co-deposited. A 100Å-Cr buffer layer was initially deposited at a substrate temperature of 600°C.[18] The substrate was then cooled to 180°C and the samples were grown by sequential deposition of the Fe and Cr layers. A similar

growth sequence has been used by Kamijo and Igarishi[19] for the growth of Fe/Cr superlattices by molecular beam epitaxy (MBE) techniques on MgO(100). Two series of samples were grown. The first was of [Fe(14Å)/Cr(t_{Cr})]$_N$ superlattices with 8<t_{Cr}<70Å and N was adjusted so that the total superlattice thickness was constant at ≈1200Å.[20] A second series of samples based on the design of Parkin and Mauri[21] was grown to measure the ferromagnetic interlayer coupling . The structure was characterized by x-ray diffraction using Cu-K_α radiation. Magnetic properties were measured by SQUID magnetometry and longitudinal Kerr rotation.

III. X-ray Diffraction

The high-angle x-ray spectra of [Fe(14Å)/Cr(46Å)]$_{20}$ superlattices grown on MgO(110) and MgO(100) substrates are shown in Figs. 1a and 1b, respectively. Figure 1a contains the MgO(220) peak and the Fe/Cr(211) reflections, and Fig. 1b contains the MgO(200) and Fe/Cr(200) reflections. There is no evidence of any other orientations present in the diffraction data. The crystalline coherence length estimated from the full width at half maximum (FWHM) of the Fe/Cr reflection K_{α_1} component is ≈400Å and 430Å for the (211) and (100) orientations, respectively. Rocking curves about the Fe/Cr reflections have FWHM that range from 0.6-1.2° for various Cr thicknesses, which is indicative of a high degree of crystal orientation. Fittings of the high-angle diffraction spectra to a general structural model[22] yield Fe and Cr lattice spacings which agree with the bulk values to better than 0.15% for both orientations.

Asymmetric diffraction scans were performed on selected samples to determine the in-plane epitaxial orientation of the superlattice with the substrate. For both orientations the (110) diffraction intensity was monitored as the sample was rotated by angle ϕ about the surface normal. The results of these scans are shown as the insets of Figs. 1a and 1b. A two- and four-fold rotational symmetry is observed for the (211) and (100) orientations, respectively, as expected. The FWHM of the ϕ-scan peaks are 1.4 and 1.0° for the (100) and (211) orientations, respectively. From the position of the peaks, the following epitaxial orientations are determined: Fe/Cr[$0\bar{1}1$] // MgO[001]for the Fe/Cr(211), and Fe/Cr[011] // MgO[001] for the Fe/Cr(100). The same epitaxial

relation Fe(211)//MgO(110) has been observed for the MBE growth of Fe(211)/Au(110) superlattices on MgO(110).[23]

IV. Magnetization

A. Antiferromagnetic coupling

The in-plane magnetization hysteresis loops were measured for the superlattices with the applied field H parallel to the Fe[$\bar{1}$11] and Fe[0$\bar{1}$1] directions for the (211) orientation and to the [011] direction for the (100) orientation. For the 14-Å Fe(211) layers, there is a strong in-plane uniaxial anisotropy along the Fe[0$\bar{1}$1] in addition to the expected crystal anisotropy. To quantify the anisotropy, we analyze the hysteresis loop of a ferromagnetically coupled sample with H along the hard axis (Fe[$\bar{1}$11]) utilizing an expression which includes a magnetocrystalline anisotropy (K_1) and a uniaxial anisotropy (K_U) along the Fe[0$\bar{1}$1], as well as a Zeeman term.[23,24] From this analysis, we have determined $K_U \approx 9 \times 10^5$ ergs/cm^3 and $K_1 \approx 4 \times 10^5$ ergs/cm^3 for the 14-Å Fe layers at room temperature. These anisotropy values are consistent with other studies of Fe(211) films.[23,24] In Refs. 23 and 24 the origin of the uniaxial anisotropy was attributed to strain. However, in our Fe/Cr superlattices, the strain appears to be quite limited. Additionally, we find that for a 90-Å Fe layer, the value of K_U decreases by an order of magnitude[20] which is consistent with the K_U term originating from a surface anisotropy.

Shown in Fig. 2a are the room-temperature hysteresis loops for AF-coupled (100)- and (211)-oriented [Fe(14Å)/Cr(26Å)]$_N$ superlattices. The effect of the in-plane anisotropy is evident in the shape and saturation fields along orthogonal directions of the (211)-superlattice. There is a clear spin-flop transition when the field is along the easy axis (Fe[0$\bar{1}$1]). When the field is along the hard axis (Fe [$\bar{1}$11]) continuous rotation to saturation is observed, which is similar to the behavior in the loop for the Fe/Cr(100) sample. As was shown by Folkerts[25], the spin-flop transition is expected to be observed for H along the easy axis when the antiferromagnetic interlayer exchange constant J_{AF} is less than $K_U t_{Fe}$.

The value of J_{AF} can be calculated from the saturation field H_S and the anisotropy constants for H applied along the easy and hard axis by the following equations from Refs. 25 and 26:

$$J_{AF}(211) = \begin{cases} \dfrac{(H_S + H_K)\, M_S\, t_{Fe}}{4} & \text{for } H \,//\, Fe[0\bar{1}1] \text{ and } J_{AF} > K_U t_{Fe} \quad (1a) \\ \dfrac{H_S\, M_S\, t_{Fe}}{2} & \text{for } H \,//\, Fe[0\bar{1}1] \text{ and } J_{AF} < K_U t_{Fe} \quad (1b) \end{cases}$$

$$J_{AF}(211) = \frac{(H_S - H_K)\, M_S\, t_{Fe}}{4} \quad \text{for } H \,//\, Fe[\bar{1}11] \quad (2)$$

$$J_{AF}(100) = \frac{(H_S - H_K)\, M_S\, t_{Fe}}{4} \quad \text{for } H \,//\, Fe[011] \quad (3)$$

$$J_{AF}(100) = \frac{(H_S + H_K)\, M_S\, t_{Fe}}{4} \quad \text{for } H \,//\, Fe[001] \quad (4)$$

where H_K is the anisotropy field given by $2K_U/M_S$ for the (211) samples, and $2K_1/M_S$ for the (100) samples. The values of H_K are estimated from the saturation fields of the ferromagnetically coupled superlattices when the field is applied along the hard axis. Applying Eqs. (1-3) to the loops shown in Fig. 2, yields $J_{AF}(211) = 0.061$ and 0.064 ergs/cm^2 for the hard and easy axis respectively and $J_{AF}(100) = 0.62$ ergs/cm^2.

Shown in Fig. 2b are the measured saturation fields for the Fe/Cr superlattices as a function of Cr layer thickness for both orientations. Four oscillations are observed with the phase and period (18Å) identical for the two orientations. To compare the interlayer coupling strengths requires converting H_S using Eqs. (1) and (3) into J_{AF} values. The calculated values for J_{AF} are shown in Fig. 2c, where H_K for both orientations were determined from the saturation field of ferromagnetically coupled samples with neighboring Cr thicknesses. We assume that any derived value of $J_{AF}<10^{-3}$ ergs/cm^2 represents either a ferromagnetic or uncoupled case and show only unambiguously AF-coupled samples in Fig. 2c. As can be seen in Fig. 2c, *in addition to the phase and period of the oscillations, the strength of the AF coupling is independent of the crystallographic orientation.*

B. Ferromagnetic coupling

To explore the coupling of the superlattice across regions where square hysteresis loops were observed for the superlattices, we have employed the structure suggested by Parkin and Mauri shown by the lower inset in Fig. 3a.[21] The 9-Å Cr layer was used to strongly AF-couple the middle Fe layer to the thicker bottom Fe layer. Monitoring the switching of the top Fe layers allows the determination of the ferromagnetic interlayer coupling. The measured Kerr intensity for the (211)-oriented sample in which the top and middle Fe layers are separated by a 19-Å Cr layers. The upper inset shows an expanded view of the low-field region. There are two switching fields observed which are labeled H_{S1} and H_{S2} in Fig. 3a, which correspond to the switching of the top and middle Fe layers, respectively. H_{S1} is related to the ferromagnetic coupling across the 19-Å Cr layer, and H_{S2} is related to the AF-coupling across the 9-Å Cr layer. The relationship between the saturation field H_{S2} and the AF interlayer coupling for strong coupling strengths is given by:[27]

$$J_{AF}(211) \approx \frac{(H_{S2} + H_K)\, M_S\, t_1}{\left(1 + \frac{t_1}{t_2}\right)} \qquad \text{for } H \,//\, Fe[0\bar{1}1] \tag{5}$$

where t_1 and t_2 correspond to the thickness of the middle and bottom Fe layers and H_K is estimated by measuring the difference in H_{S2} along both the easy and hard directions. For samples with $t_2 >> t_1$, the saturation field will be roughly 1/4 that of the corresponding superlattice with magnetic layer thicknesses t_1. The ferromagnetic coupling strength when H is along the easy axis is given by:

$$J_F(211) = H_{S1} M_S\, t_{Fe} \qquad \text{for } H \,//\, Fe[0\bar{1}1] \text{ and } J_F < 2K_U t_{Fe}\,. \tag{6}$$

There are equivalent expressions for the (100) orientations. For the sample shown in Fig. 3a, J_{AF} determined from Eq. (5) is 0.9 ergs/cm^2, which is consistent with the superlattice results for comparable Cr thicknesses in Fig 2c. Shown in Fig. 3b is the interlayer coupling measured from 8 to 32Å Cr showing the coupling oscillating about zero for both orientations. This result is in

quantitative agreement to that of Grünberg *et al.*[28] for the long-period oscillation across a Cr(100) wedge.

V. Conclusion

The short-period (two monolayers) oscillations observed in Fe/Cr(100)/Fe wedged samples are thought to be directly related to the nested Fermi surface of Cr which gives rise to the spin-density wave in Cr.[3,4] The origin of the 18-Å long-period oscillation is not as easily related to the magnetic properties of Cr. Stiles[8] has shown that there are a number of spanning vectors in Cr (100), (110) and (111) orientations which could give rise to long-period oscillations. However, it is not understood within this theoretical framework which of the many spanning vector will give rise to the coupling. Unlike the period of the coupling, which is thought to be intrinsic to the interlayer material, the strength and phase of the coupling depends on the matrix elements in the numerator of the RKKY expressions,[5-12] the ferromagnetic material,[9] and the structure of the interface.[7] In general, it is expected that the strength, phase, and period of the coupling should be strongly dependent on the crystal orientation. Given this expectation, the results in Figs. 2 and 3 showing no difference between the (100) and (211) oriented samples is surprising. In addition to the orientations studied in this paper, oscillations in the AF coupling has been observed with the same phase and period and similar coupling strengths in (110) textured multilayers.[29] At present, all of the studies of the Fe/Cr system which show oscillatory behavior have found the same 18Å long-period oscillation.

In conclusion , we have grown epitaxial Fe/Cr(100) and (211) superlattices on MgO(100) and (110) substrates respectively. Both orientation show interlayer coupling which oscillates from antiferromagnetic to ferromagnetic with a period of 18Å. The phase, period, strength of the coupling is found to be independent of the crystallographic orientation.

The work was supported by the U.S. Department of Energy, Basic Energy Sciences-Materials Sciences, under contract W-31-109-ENG-38.

References

1. P. Grünberg, R. Schreiber, Y. Pang, M. B. Brodsky, and C.H. Sowers, Phys. Rev. Lett. **57**, 2442 (1986).
2. S.S.P. Parkin, N. More, and K. P. Roche, Phys. Rev. Lett. **64**, 2304 (1990).
3. J. Unguris, R. J. Celotta, D. T. Pierce, Phys. Rev. Lett. **67**, 140 (1991).
4. S.T. Purcell, W. Folkerts, M.T. Johnson, N.W.E. McGee, K. Jager, J. aan de Stegge, W.B. Zeper, W.. Hoving, P. Grünberg, Phys. Rev. Lett. **67**, 903 (1991).
5. Y. Wang, P.M. Levy, and J.L. Fry, Phys. Rev. Lett. **65**, 2732 (1990).
6. P. Bruno and C. Chappert, Phys. Rev. Lett. **67**, 1602 (1991); Phys. Rev. B **46**, 261 (1992).
7. F. Herman and R. Schrieffer, Phys. Rev. B **46**, 5806 (1992).
8. M. D. Stiles, (unpublished).
9. J. Mathon, M. Villere, and D. M. Edwards, J. Phys: Condens. Matter **4**, 9873 (1992).
10. R.P. Erickson, K.B. Hathaway, and J.R. Cullen, Phys. Rev. B **47**, 2626 (1993).
11. R. Coehoorn, Phys. Rev. B **44**, 933 (1991).
12. E. Bruno and B.L. Gyorffy, Phys. Rev. Lett. **71**, 181 (1993).
13. S.S.P. Parkin, R. Bhadra, and K.P. Roche, Phys. Rev. Lett. **66**, 2152 (1991).
14. M.T. Johnson, R. Coehoorn, J.J. de Vries, N.W.E. McGee, J. ann de Stegge, and P.J.H. Bloemen, Phys. Rev. Lett. **69**, 969 (1992).
15. Z.Q. Qiu, J. Pearson, and S.D. Bader, Phys. Rev. B **46**, 8659 (1992).
16. A. Schreyer, K. Bröhl, J.F. Ankner, C.F. Majkrzak, Th. Zeidler, P. Bödeker, N. Metoki, and H. Zabel, Phys. Rev. B **47**, 15334 (1993).

17. S.N. Okuno and K. Inomata, Phys. Rev. Lett. **70**, 1711 (1993).

18. B.M. Lairson, M.R. Visokay, R. Sinclair, and B.M. Clemens, Appl. Phys. Lett. **61**, 1390 (1992).

19. A. Kamijo and H. Igarishi, J. Appl. Phys. **71**, 2455 (1992).

20. E. E. Fullerton, M.J. Conover, J.E. Mattson, C.H. Sowers, and S.D. Bader, Phys. Rev. B, submitted (1993).

21. S.S.P. Parkin and D. Mauri, Phys. Rev. B **44**, 7131 (1991).

22. E.E. Fullerton, I.K. Schuller, and Y. Bruynseraede, MRS Bulletin **XVII**(12), 33 (1992); E.E. Fullerton, I. K. Schuller, H. Vanderstraeten, and Y. Bruynseraede, Phys. Rev. B **45**, 9292 (1992).

23. A. Marty, B. Gilles, J. Eymery, A. Chamberod, and J.C. Joud, J. Magn. Magn. Mater. **121**, 57 (1993).

24. Y. Ueda and M. Takahashi, J. Magn. Magn. Mater. **71**, 212 (1988).

25. W. Folkerts, J. Magn. Magn. Mater. **94**, 302 (1991).

26. W. Folkerts and F. Hakkens, J. Appl. Phys. **73**, 3922 (1993).

27. W. Folkerts and S.T. Purcell, J. Magn. Magn. Mater. **111**, 306 (1992).

28. S. Demokritov, J.A. Wolf, and P. Grünberg, Europhys. Lett. **15**, 881 (1991).

29. S.S.P. Parkin, N. More, and K. P. Roche, Phys. Rev. Lett. **64**, 2304 (1990).

Figure Captions

Figure 1: X-ray diffraction results for Fe/Cr superlattices grown on MgO. High-angle spectra for $[Fe(14Å)/Cr(46Å)]_{20}$ superlattices grown on (a) MgO(110) and (b) MgO(100). Arrows at the top identify the position of possible Fe/Cr reflections. The MgO reflections are also identified. The insets show the Fe/Cr (110) intensity as a function of rotation angle ϕ about the surface normal for $[Fe(14Å)/Cr(17Å)]_{36}$ superlattices grown on (a) MgO(110) and (b) MgO(100).

Figure 2: (a) Room-temperature magnetic hysteresis loops for (100)- and (211)-oriented $[Fe(14Å)/Cr(26Å)]_N$ superlattices. The applied field is along the Fe[011] direction for the (100) superlattice and along the easy Fe[$0\bar{1}1$] and hard Fe[$\bar{1}11$] directions for the (211) superlattice. (b) Switching field H_S for (211)- and (100)-oriented $Fe(14Å)/Cr(t_{Cr})$ superlattices measured at room temperature with H parallel to the Fe[$0\bar{1}1$] direction. (b) Antiferromagnetic coupling strength J_{AF} *vs* t_{Cr} for (211)- and (100)-oriented $Fe(14Å)/Cr(t_{Cr})$ superlattices determined from H_S values shown in (b)

Figure 3: .(a) Room-temperature hysteresis loop measured by Kerr rotation of a (211)-oriented Fe(100Å)/Cr(9Å)/Fe(20Å)/Cr(19Å)/Fe(20Å)/Cr(20Å) sample. The arrows indicate the magnetization diretions of the three Fe layers. The inset shows an expanded view of the low-field region. (b) Interlayer coupling J *vs* t_{Cr} for (211)- and (100)-oriented samples, where antiferromagnetic coupling ($J < 0$) was determined from the superlattices and ferromagnetic coupling ($J > 0$) was determined from the samples shown schematically in (a). Note the change in scale at t_{Cr}=15Å.

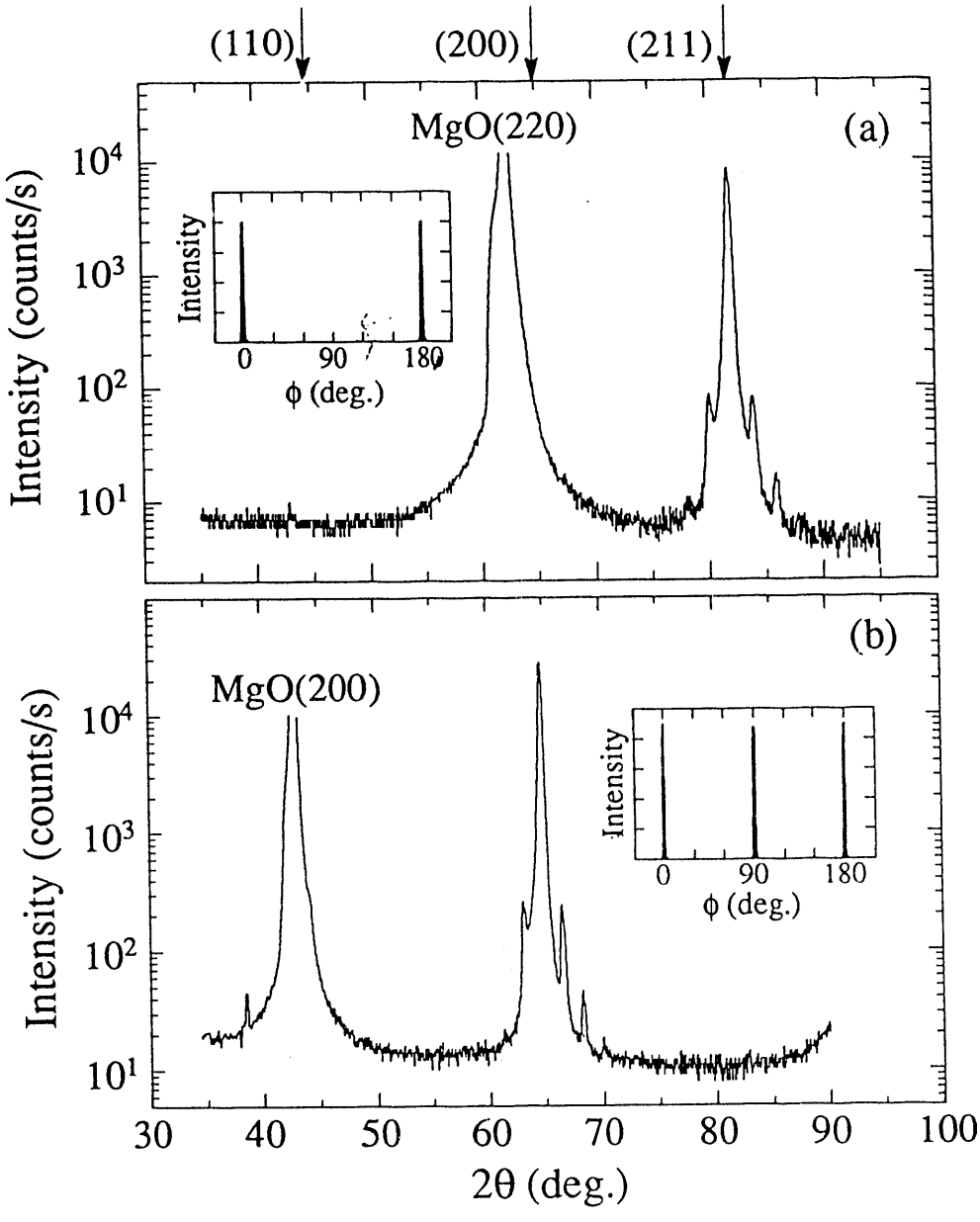

Fullerton *et al.*
EP-14
Fig. 1 of 3

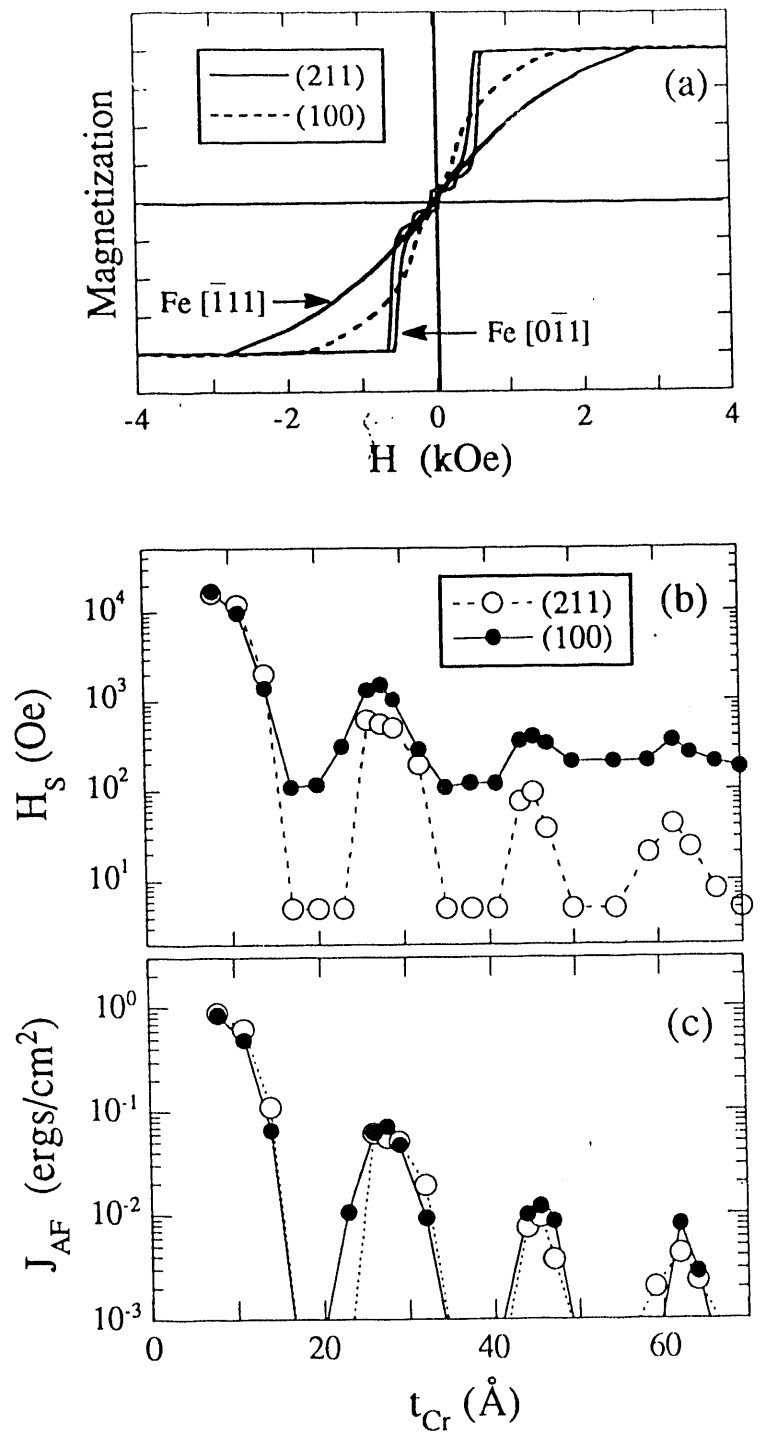

Fullerton *et al.*
EP-14
Fig. 2 of 3

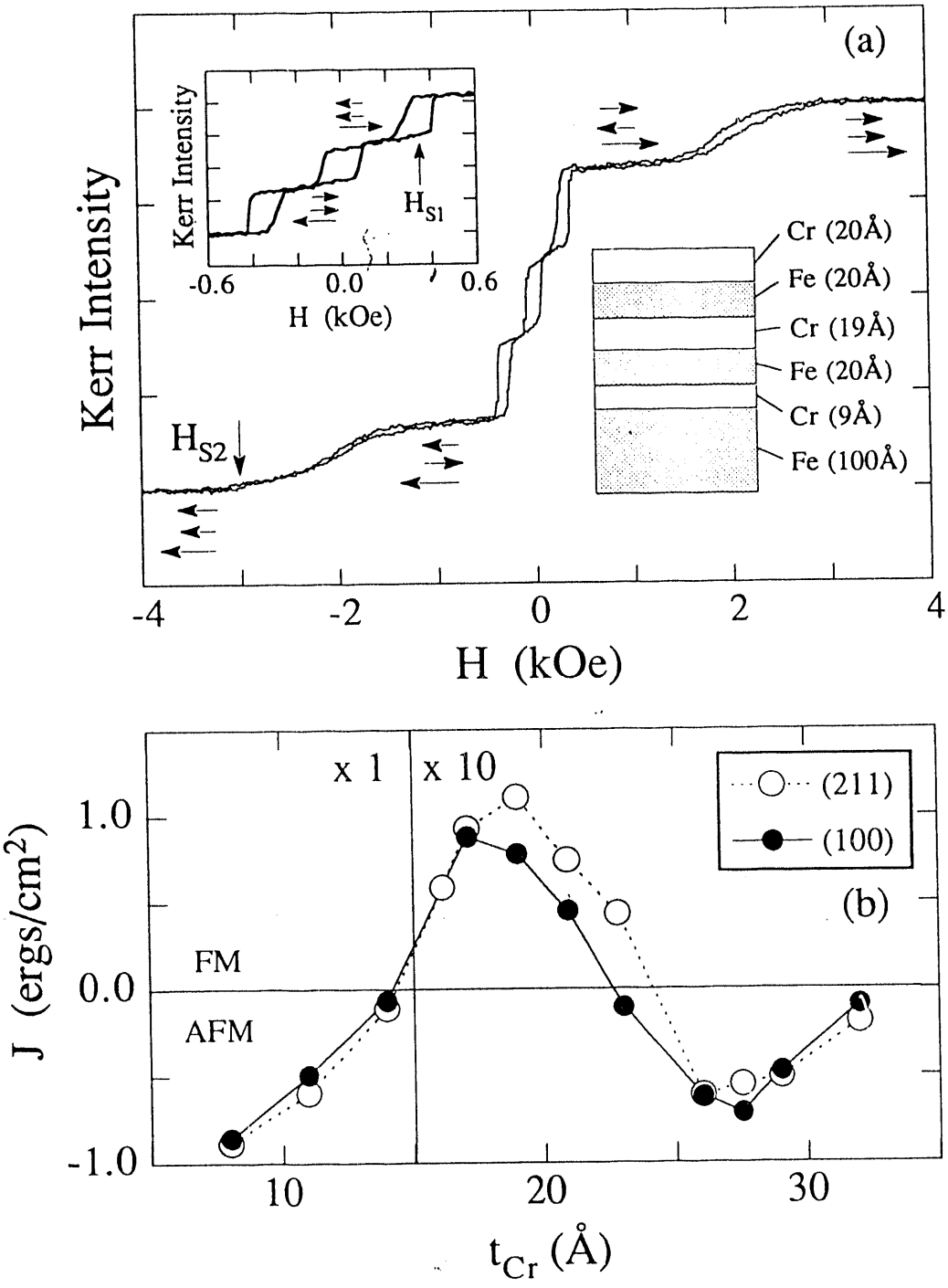

Fullerton *et al.*
EP-14
Fig. 3 of 3

DATE
FILMED
12/8/93
END